

Impact of the 2019/2020 Australian megafires on air quality and health

Ailish M. Graham, Kirsty J. Pringle, Richard J. Pope, Stephen R. Arnold, Luke A. Conibear, Helen Burns, Richard Rigby, Nicolás Borchers-Arriagada, Edward W. Butt, Laura Kiely, Carly Reddington, Dominick V. Spracklen, Matthew T. Woodhouse, Christoph Knotte, James B. McQuaid

Angaben zur Veröffentlichung / Publication details:

Graham, Ailish M., Kirsty J. Pringle, Richard J. Pope, Stephen R. Arnold, Luke A. Conibear, Helen Burns, Richard Rigby, et al. 2021. "Impact of the 2019/2020 Australian megafires on air quality and health." *GeoHealth* 5 (10): e2021GH000454. <https://doi.org/10.1029/2021gh000454>.

Impact of the 2019/2020 Australian Megafires on Air Quality and Health



Key Points:

- The fires led to widespread exposure to “Poor” or worse Air Quality Index levels across eastern-Australia
- The highest all-cause, all-age mortality from short-term exposure to bushfire particulate matter with a diameter less than $2.5 \mu\text{m}$ ($\text{PM}_{2.5}$) was seen in the states of New South Wales, Queensland, and Victoria
- All-cause, all-age mortality from short-term exposure to bushfire $\text{PM}_{2.5}$ was highest in the cities of Sydney, Melbourne, and Canberra

Supporting Information:

Supporting Information may be found in the online version of this article.

Correspondence to:

A. M. Graham,
ee15amg@leeds.ac.uk

Citation:

Graham, A. M., Pringle, K. J., Pope, R. J., Arnold, S. R., Conibear, L. A., Burns, H., et al. (2021). Impact of the 2019/2020 Australian megafires on air quality and health. *GeoHealth*, 5, e2021GH000454. <https://doi.org/10.1029/2021GH000454>

Received 13 MAY 2021

Accepted 7 OCT 2021

Author Contributions:

Conceptualization: Ailish M. Graham












Data curation: Ailish M. Graham, Edward W. Butt

Formal analysis: Ailish M. Graham

Investigation: Ailish M. Graham

Methodology: Ailish M. Graham

Resources: Nicolás Borchers-Arriagada, Laura Kiely, Carly Reddington, Dominick V. Spracklen, Matthew T. Woodhouse

Ailish M. Graham¹ , Kirsty J. Pringle¹ , Richard J. Pope^{1,2} , Stephen R. Arnold¹ , Luke A. Conibear¹ , Helen Burns^{1,3} , Richard Rigby^{1,3} , Nicolás Borchers-Arriagada⁴, Edward W. Butt¹ , Laura Kiely¹, Carly Reddington¹ , Dominick V. Spracklen¹, Matthew T. Woodhouse⁵ , Christoph Knote⁶, and James B. McQuaid¹ 

¹School of Earth and Environment, University of Leeds, Leeds, UK, ²National Centre for Earth Observation, University of Leeds, Leeds, UK, ³Centre for Environmental Modelling and Computation, University of Leeds, Leeds, UK, ⁴Menzies Institute for Medical Research, University of Tasmania, Hobart, TAS, Australia, ⁵Commonwealth Scientific and Industrial Research Organisation, Aspendale, VIC, Australia, ⁶Model-Based Environmental Exposure Science, Faculty of Medicine, University of Augsburg Germany, Augsburg, Germany

Abstract The Australian 2019/2020 bushfires were unprecedented in their extent and intensity, causing a catastrophic loss of habitat, human and animal life across eastern-Australia. We use a regional air quality model to assess the impact of the bushfires on particulate matter with a diameter less than $2.5 \mu\text{m}$ ($\text{PM}_{2.5}$) concentrations and the associated health impact from short-term population exposure to bushfire $\text{PM}_{2.5}$. The mean population Air Quality Index (AQI) exposure between September and February in the fires and no fires simulations indicates an additional $\sim 437,000$ people were exposed to “Poor” or worse AQI levels due to the fires. The AQ impact was concentrated in the cities of Sydney, Newcastle-Maitland, Canberra-Queanbeyan and Melbourne. Between October and February 171 (95% CI: 66–291) deaths were brought forward due to short-term exposure to bushfire $\text{PM}_{2.5}$. The health burden was largest in New South Wales (NSW) (109 (95% CI: 41–176) deaths brought forward), Queensland (15 (95% CI: 5–24)), and Victoria (35 (95% CI: 13–56)). This represents 38%, 13% and 30% of the total deaths brought forward by short-term exposure to all $\text{PM}_{2.5}$. At a city-level 65 (95% CI: 24–105), 23 (95% CI: 9–38) and 9 (95% CI: 4–14) deaths were brought forward from short-term exposure to bushfire $\text{PM}_{2.5}$, accounting for 36%, 20%, and 64% of the total deaths brought forward from all $\text{PM}_{2.5}$. Thus, the bushfires caused substantial AQ and health impacts across eastern-Australia. Climate change is projected to increase bushfire risk, therefore future fire management policies should consider this.

Plain Language Summary The Australian 2019/2020 bushfires were unprecedented in their size and intensity, resulting in a catastrophic loss of habitat and human and animal life across eastern-Australia. We use an air pollution model (WRF-Chem) to quantify the impact of the bushfires on particulate matter with a diameter less than $2.5 \mu\text{m}$ ($\text{PM}_{2.5}$) concentrations. We run the model with and without emissions from the fires so their impact on $\text{PM}_{2.5}$ can be isolated. We find that between September and February an additional $\sim 437,000$ people were exposed to “Poor” or worse air quality index levels due to the fires across eastern-Australia. Short-term exposure to high $\text{PM}_{2.5}$ concentrations has been linked to negative health impacts. Therefore, we estimate the health impact of population exposure to bushfire $\text{PM}_{2.5}$ across eastern-Australia, regionally and at city level. Our estimate indicates that between October and February 171 deaths were brought forward due to exposure to $\text{PM}_{2.5}$ from the fires. Regionally, most deaths were brought forward in New South Wales (109 deaths brought forward), Queensland (15), and Victoria (35). Within these regions, the most deaths were brought forward in Sydney (65), Melbourne (23), and Canberra-Queanbeyan (9) as large populations were exposed to high $\text{PM}_{2.5}$ concentrations due to the bushfires.

1. Introduction

The Australian 2019/2020 bushfires were unprecedented in both their extent and intensity (Brew et al., 2020), causing a catastrophic loss of habitat and human and animal life. Between October 2019 and February 2020 hundreds of fires burned in the south-east of the country, peaking in size in December and

Software: Ailish M. Graham, Luke A. Conibear, Helen Burns, Richard Rigby, Christoph Knotz
Supervision: Stephen R. Arnold
Validation: Ailish M. Graham
Visualization: Ailish M. Graham
Writing – original draft: Ailish M. Graham
Writing – review & editing: Ailish M. Graham

January. By burned area the bushfires were the largest in south-east Australia since European occupation (late 1700s) (Wintle et al., 2020), burning more than 10 million hectares of vegetation. The burned area of the 2019/2020 fires was larger than the Ash Wednesday (1983) and Black Saturday (2009) fires combined (Brew et al., 2020). The immediate impacts of the bushfires included the destruction of almost 6,000 buildings and the deaths of 34 people and more than 3 billion terrestrial vertebrates (Verzoni, 2021).

The severity of the 2019/2020 bushfire season was promoted by a decrease in rainfall and increase in temperatures due to a combination of meteorological and climatic conditions (Australian Bureau of Meteorology, 2019a). Australia had experienced two consecutive very dry years prior to 2019 (2017–2018), with 2019 being the warmest and driest on record (van Oldenborgh et al., 2020). This was combined with a strong positive Indian Ocean Dipole (IOD) phase from July 2019 onwards (Australian Bureau of Meteorology, 2020) and a negative Southern Annular Mode (SAM) event (Australian Bureau of Meteorology, 2019b), both of which reduce rainfall across south-eastern Australia.

Climate change is projected to increase the frequency, intensity and spread of wildfires both globally (Sutton et al., 2011) and in Australia (Lucas et al., 2007). Fire weather conditions in Australia are predicted to worsen, with forest fire danger index (FFDI) projected to increase in all climate change scenarios (0%–30% by 2050) (Lucas et al., 2007). Alongside this, the number of days where fire danger is “very-high” or “extreme” is projected to increase, with an increase in the length of the fire season (Lucas et al., 2007). The largest changes in FFDI are predicted to be seen in New South Wales due to the Mediterranean climate of the region. Mild, wet winters encourage the growth of fuel, and hot, dry summers lead to an increase in the FFDI (Lucas et al., 2007). The increase in bushfire frequency and intensity is likely to increase population exposure to pollutants from bushfires, and therefore the health burden of bushfire events.

Substantial epidemiological and toxicological evidence supports the association between wildfire $PM_{2.5}$ exposure and short-term all-cause mortality and short-term respiratory morbidity (Delfino et al., 2009; Faustini et al., 2015; Johnston et al., 2011; Naeher et al., 2007; Reid et al., 2016; Zanobetti & Schwartz, 2009). However, research to identify the toxicity of different components of $PM_{2.5}$ chemical composition is ongoing, and so equal toxicity for all $PM_{2.5}$ is commonly assumed in health impact assessments. The health burden of wildfires is concentrated in the tropics, Australia, Canada, and the USA and is substantial (Black et al., 2017; Crippa et al., 2016; Johnston et al., 2012; Liu et al., 2015; Reid et al., 2016). The effect of wildfires on $PM_{2.5}$ concentrations in these countries is so large that the $PM_{2.5}$ associated health burden from long-term exposure is dominated by exposure to wildfires in large parts of them (Lelieveld et al., 2015). Therefore, reducing population exposure to pollutants from wildfires is likely to yield large near-term health benefits in these regions (Johnston et al., 2012).

Two studies have previously estimated the impacts of the 2019/2020 bushfires on mortality due to short-term exposure to bushfire $PM_{2.5}$. Both studies used observational data from the ground-based monitoring network in south-east Australia to estimate daily mean $PM_{2.5}$ exposure. The first study, from Borchers Ariagada et al. (2020), estimated exposure using inverse distance weighting to interpolate $PM_{2.5}$ monitoring data spatially to statistical area level 2 (SA2s) centroids within 100 km of each monitoring site. The entire SA2 population was then assumed to be exposed to the interpolated $PM_{2.5}$ concentration. Bushfire smoke affected days were defined, for each monitoring site, as days where the daily mean $PM_{2.5}$ concentration exceeded the 95th percentile of historical daily mean $PM_{2.5}$ concentrations. The contribution of bushfire smoke to the total $PM_{2.5}$ mass (bushfire smoke $PM_{2.5}$) was estimated using the difference between the observed $PM_{2.5}$ concentration and the long-term historical monthly mean $PM_{2.5}$ concentration at each monitoring site. Using the bushfire smoke $PM_{2.5}$ fraction the health impacts of bushfire $PM_{2.5}$ exposure were estimated, applying the World Health Organisation (2013) short-term exposure-response function for all-cause, all-age mortality. The estimated health impact on mortality was substantial, with an estimated 417 (95% CI: 153–680) deaths brought forward across eastern-Australia due to short-term exposure to bushfire smoke between October 1, 2019 and February 10, 2020. The health impact was highest in New South Wales and Victoria, with 219 (95% CI: 81–357) and 120 (95% CI: 44–195) deaths brought forward by bushfire $PM_{2.5}$.

In a separate study, Ryan et al. (2021) used a random forest model, trained using historical ground-based observations, to predict air pollutant concentrations, including $PM_{2.5}$, without bushfires. These estimates were compared with ground-based observations during the period of the bushfires to estimate the bushfire

contribution to $PM_{2.5}$ concentrations each day. Population-weighted bushfire $PM_{2.5}$ exposure and mortality from short-term exposure to bushfire $PM_{2.5}$ in New South Wales and Victoria were then estimated in the same way as Borchers Arriagada et al. (2020). The estimated health impact lay within the lower limit of Borchers Arriagada et al. (2020) in New South Wales and Victoria at 152 (95% CI: 95–209) and 92 (95% CI: 57–126) deaths brought forward due to bushfire $PM_{2.5}$, compared with 219 (95% CI: 81–357) and 120 (95% CI: 44–195). The difference was attributed to the different approaches to quantifying the bushfire fraction of $PM_{2.5}$, as well as the study by Ryan et al. (2021) only including populations within the large cities (~80% of the region), rather than the entire region.

This study will use an atmospheric chemistry transport model (ACTM) to explicitly simulate $PM_{2.5}$ concentrations with and without bushfires between September 1, 2019 and January 31, 2020 at 30 km resolution. This method aims to provide a more accurate daily estimation of the bushfire smoke contribution to total $PM_{2.5}$ mass, by simulating $PM_{2.5}$ concentrations accounting for real time meteorological conditions and atmospheric processes, and calculating explicitly the $PM_{2.5}$ increment due to the fires. Regional population exposure is likely to be better captured, since this is more challenging to capture using the sparse monitoring network, which may not capture strong $PM_{2.5}$ concentration gradients that are likely to have occurred during the fires. The use of an ACTM also allows us to estimate the health impacts of bushfire $PM_{2.5}$ exposure at both city and region (state)-wide scales. Region and city-scale AQ and health impact estimates can help governments to focus future policies toward particularly fire vulnerable regions based on the health benefits that are likely to be seen by reducing population exposure.

2. Materials and Methods

2.1. Model Description

$PM_{2.5}$ concentrations between September 1, 2019 and January 31, 2020 were simulated using the Weather Research and Forecasting model coupled to Chemistry (WRF-Chem) model (version 3.7.1), a fully coupled atmospheric chemistry model. A detailed model description can be found in Conibear et al. (2018a), and this model version has been used to successfully simulate $PM_{2.5}$ air pollution for India (Conibear et al., 2018a, 2018b, 2018c), SE Asia (Kiely et al., 2019, 2020), and China (Reddington et al., 2019; Silver et al., 2020). The model domain covered eastern-Australia (128.9–170.6°E and 9 to 48°S) at 30 km horizontal resolution (130 x 150 grid boxes), with 33 vertical levels (up to 10 hPa) and included 89% (22.1 m) of the Australian population. The contribution of bushfires to surface $PM_{2.5}$ concentrations between September 1 and January 31 was calculated by simulating two scenarios, with and without fire emissions. This allowed the contribution of the fires to air quality and health be quantified ($PM_{2.5 \text{ Fires}} - PM_{2.5 \text{ No Fires}} = PM_{2.5 \text{ Fires Only}}$).

Meteorological conditions were initialized using ERA5 6-hr analyses at 0.1° resolution on 38 pressure levels (Hoffmann et al., 2018). Nudging was used in order to keep simulated meteorology in line with the meteorological analyses. Several nudging sensitivity experiments were carried out to investigate the sensitivity of simulated $PM_{2.5}$ concentrations to the nudging option used (Table S1 in Supporting Information S1). Nudging of potential temperature, the horizontal and vertical winds and the water vapor mixing ratio in all vertical levels, rather than just above the boundary layer, improved simulated $PM_{2.5}$ concentrations by reducing the Root Mean Square Error (RMSE) to 24.1 $\mu\text{g m}^{-3}$ from 25.7 $\mu\text{g m}^{-3}$, Normalised Mean Absolute Error (NMAE) to 0.65 from 0.70 and Normalised Mean Bias (NMB) to -0.24 from -0.53, and the Pearson correlation coefficient (r) to 0.53 from 0.48, respectively (Table S1 in Supporting Information S1). Therefore, the results of the simulations where all meteorological variables in all vertical levels were nudged are presented here.

Chemical boundary conditions were provided by the Whole Atmosphere Community Climate Model (WACCM) 6-hourly simulation data (Marsh et al., 2013; UCAR, 2020a). WACCM meteorology is driven by the NASA Global Modeling and Assimilation Office (GMAO) Goddard Earth Observing System Model (GEOS-5) model. Anthropogenic emissions for 2014 from the Community Emissions Data System (CEDS) (used in the 6th Coupled Model Intercomparison Project (CMIP6)) and the Fire Inventory from NCAR (FINN) version 1 (v1) fire emissions are used in WACCM. Model output is given on 88 vertical levels at $0.9 \times 1.25^\circ$ (UCAR, 2020b).

Global anthropogenic emissions were taken from the Emission Database for Global Atmospheric Research with Task Force on Hemispheric Transport of Air Pollution version 2.2 (EDGAR-HTAP2) (Janssens-Maenhout et al., 2015) at 0.1° resolution for 2010. Sector specific diurnal cycles were subsequently added to the emissions, using diurnal cycles from Olivier et al. (2003). EDGAR-HTAP2 is a global, gridded, air pollution emission inventory compiled of officially reported, national gridded inventories. Where national emissions datasets or specific sectors are not available 2010 EDGAR v4.3 grid maps are used. Emissions include SO₂, NO_x, CO, NMVOC, NH₃, PM₁₀, PM_{2.5}, BC, and OC. Emissions include all anthropogenic emissions except large-scale biomass burning (e.g., wildfires).

The Model for Ozone and Related Chemical Tracers, version 4 (MOZART-4) (Emmons et al., 2009) is used to calculate gas-phase chemical reactions. Aerosol chemistry and physics are represented using the Model for Simulating Aerosol Interactions and Chemistry (MOSAIC) scheme, with sub-grid scale aqueous chemistry (Zaveri et al., 2008). Aerosols are represented by four sectional discrete size bins (0.039–0.156, 0.156–0.625, 0.625–2.5, and 2.5–10). The use of the MOSAIC scheme with four size bins balances detailed chemistry with computational expense.

2.1.1. Wildfire Emissions

Wildfire emissions are taken from FINNv1 near-real time (FINNv1 NRT), since FINNv1.5 was not available at the time model simulations were carried out. FINN combines satellite observations, land cover, biomass consumption estimates and emissions factors to calculate daily fire emissions globally at 1 km resolution. FINN uses satellite observations from the MODIS Thermal Anomalies Product to provide detections of active fires. Burned area is assumed to be 1 km² for each fire identified and scaled back based on the density of vegetation from the MODIS Continuous Fields (VCF) (i.e., if 50% bare = 0.5 km² burned area). The type of vegetation burned during a detected fire is determined using the MODIS Collection 5 Land Cover Type (LCT). This assigns each fire pixel to one of 16 possible land cover/land use classes and also the density of vegetation at 500 m resolution, scaled to 1 km. The 16 LCTs are then aggregated into 8 generic categories to which fuel loadings are applied (Wiedinmyer et al., 2011). Fuel loadings are from Hoelzemann et al. (2004) and emissions factors are from Akagi et al. (2011), Andrae and Merlet (2001), and McMeeking (2008). Fire types included are wildfires, prescribed and agricultural burning. However, trash burning or biofuel use are not included.

The key difference between FINN v1 NRT and FINN v1.5 is that FINN v1 NRT uses MODIS near real time fire counts rather than the reprocessed fire counts, which FINN v1.5 uses. The differences between the two datasets over Australia for the year 2018 (and 2019 following the v1.5 release) are quantified (Figure S1 in Supporting Information S1) to identify any differences in emissions. Generally, emissions for 2019 indicate that emissions per fire hotspot were much higher than previous years (2010–2018). This is likely due to the high levels of dry fuel availability during 2019 (van Oldenborgh et al., 2020). Emissions in FINN v1.5 and NRT are in good agreement for 2018, while for 2019 FINN NRT PM_{2.5} (~1 Tg) are slightly higher than FINNv1.5 (~0.9 Tg). However, there is a much larger range of disagreement in the estimates of 2019 annual fire emissions between the five key fire emissions datasets (~1–>7.5 Tg) (Figure S2 in Supporting Information S1). Due to the large discrepancies in annual fire emission estimates from the five key fire emission datasets available, we also carry out a further simulation where FINN NRT emissions are scaled by 1.5 (referred to later as scaled_1.5) to test the sensitivity of simulated PM_{2.5} concentrations to total fire emissions.

2.1.2. Release of Fire Emissions

The high temperatures associated with combustion mean that wildfires can often inject emissions above the surface due to buoyancy of the fire plume. In WRF-Chem a default plume-rise parameterization is used to release fire emissions (Freitas et al., 2007). However, several studies have found that the plume-rise parameterization potentially represents an incorrect vertical distribution of the emissions (Archer-Nicholls et al., 2015; Crippa et al., 2016). Kiely et al. (2020, 2019) found that releasing emissions evenly through the boundary layer (BL) improved agreement between simulated surface PM_{2.5} concentration and observations for Indonesian fires. Therefore, we test two options: (a) releasing emissions evenly through the boundary layer and (b) plume-rise. The results of this sensitivity study indicate that simulated PM_{2.5} concentrations are relatively insensitive to the emission option used (Figure S4 and Table S1 in Supporting Information S1).

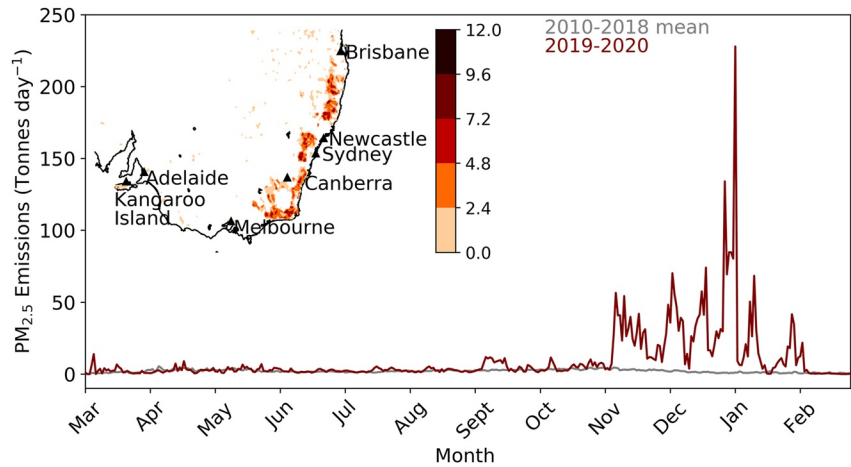


Figure 1. Particulate matter with a diameter less than $2.5 \mu\text{m}$ ($\text{PM}_{2.5}$) fire emissions (Tonnes day^{-1}) across Australia between March 2019 and March 2020 from the FINN near-real time fire emission data set. The timeseries shows the 2010–2018 daily mean $\text{PM}_{2.5}$ emissions (gray) and the 2019–2020 daily mean $\text{PM}_{2.5}$ emissions (maroon). Inset map: Total $\text{PM}_{2.5}$ fire emissions (Tonnes km^{-2}) across eastern Australia between March 2019 and March 2020.

but releasing emissions evenly through the BL performs better. Therefore, we present the results of releasing emissions evenly through the BL in this study.

2.2. Observations

2.2.1. Ground-Based Monitoring Sites

Daily mean $\text{PM}_{2.5}$ mass concentrations, calculated from hourly $\text{PM}_{2.5}$ observations, at ground-based monitoring sites are used to assess model performance in simulating $\text{PM}_{2.5}$ concentrations. Data from the New South Wales, Queensland, Australian Capital Territory Government, and the Victoria EPA monitoring networks were combined, providing data across 80 observational sites. A map of sites used is available in the Supporting Information S1 (Figure S3 in Supporting Information S1). Daily means were calculated from hourly data if > 18 hr of data was available each day, otherwise a missing data flag was applied. Model performance was evaluated using r , NMB, RMSE, and NMAE (Table S1 in Supporting Information S1). Multiple observations were available in several large cities (Newcastle, Sydney, Canberra, Melbourne—see Figure 1 for locations), allowing the model performance to be evaluated in locations where populations are likely to have been exposed to high concentrations of $\text{PM}_{2.5}$.

2.2.2. Health Impact Assessment

In order to assess the exposure of populations in individual regions and cities, population-weighted bushfire $\text{PM}_{2.5}$ concentrations are used. Population data is separated by region and city using shapefiles and then population-weighted $\text{PM}_{2.5}$ concentrations are calculated (Equation 1). The population and concentration in each grid box (pop_i and conc_i) are summed and divided by the total population (pop) in the region/city.

$$\text{Population_weighted PM}_{2.5} = \frac{\sum(\text{pop}_i \times \text{conc}_i)}{\sum \text{pop}} \quad (1)$$

All-cause, all-age mortality from short-term exposure to $\text{PM}_{2.5}$ is calculated using a concentration-response function (CRF). We use relative risk values from the World Health Organisation (2013) of 1.0123 (95% CI: 1.0045, 1.0201) per $10 \mu\text{g m}^{-3}$, which we use to estimate beta (β) using Equation 2. Since the RR used is for all-cause, all-age mortality, we use all-cause, all-age baseline mortality rates in the calculations.

$$\beta = \frac{\ln(\text{RR})}{\Delta C} \quad (2)$$

The AF (Equation 4) is calculated using the concept of relative risk (RR) (Equation 3), which is the probability of mortality from a disease endpoint within an exposed population compared to within an unexposed population. The concentration of bushfire PM_{2.5} that a population is exposed to is given by ΔX (PM_{2.5} FIRES – PM_{2.5} NO FIRES) and the safe-limit of exposure is X_0 (Equation 3). Since there is little evidence to suggest a safe-limit of exposure to PM_{2.5} we assume X_0 to be zero (Holgate, 1998; Macintyre et al., 2016; Schmidt et al., 2011).

$$RR = \exp^{\beta(\Delta X - X_0)} \quad (3)$$

$$AF = \left(\frac{RR - 1}{RR} \right) \quad (4)$$

The excess mortality caused by exposure to PM_{2.5} over the theoretical minimum risk level of exposure (Equation 3: $\Delta X - X_0$) each day is represented by E_m . N is the number of days within the simulation and i is the day in simulation (Equation 5), B_d is the baseline death rate, pop_i is the population exposed each day and AF_i is the attributable fraction of risk each day due to exposure to PM_{2.5} (calculated in Equation 4).

$$E_m = \sum_{i=1}^N B_d \cdot pop_i \cdot AF_i \quad (5)$$

Health impacts are calculated at 1 km resolution to match the resolution of the population data and separated by region and city using shapefiles.

2.2.3. Population and Baseline Mortality Data

Population count data for 2018 is from the Australia Bureau of Statistics (Australian Bureau of Statistics, 2019) at 1 km resolution. This indicates our model domain includes 89% of the Australian population. Baseline all-cause, all-age 2018 mortality rate data for each region in our model domain is taken from the Australia Bureau of Statistics (Australian Bureau of Statistics, 2020) (Table S4 in Supporting Information S1).

3. Results

3.1. Fire Emissions

FINN emissions clearly indicate that the PM_{2.5} emissions between late-October 2019 and mid-January 2020 were unprecedented, lying far above the daily mean emissions observed in the previous 8 years (Figure 1 and Figure S1 in Supporting Information S1). The Australian bushfires in 2019–2020 began in the northern region of eastern-Australia (close to Brisbane and Newcastle) and shifted south through the season (Figure 1). As the fires moved southwards, PM_{2.5} emissions also increased, with the highest PM_{2.5} emissions occurring in south-eastern Australia in late December-early January.

The impact of the fires on PM_{2.5} air quality (AQ) is clear from ground-based observations across south-east Australia (Figure 2). Observations indicate that between October 2019 and February 2020 daily mean PM_{2.5} concentrations averaged across all sites reached 70 $\mu\text{g m}^{-3}$ on several days. In the no fires simulation concentrations remain below 20 $\mu\text{g m}^{-3}$, indicating that a large fraction of the total PM_{2.5} mass observed is due to fires. The impact of the fires on populations can be more clearly seen when PM_{2.5} concentrations in individual cities are examined (Figure 2). Newcastle and Sydney exhibit the same pattern of PM_{2.5} variability, following the pattern seen regionally across eastern-Australia closely. High PM_{2.5} concentrations are first observed in late October and affect the cities sporadically until mid-January, reaching $\sim 75 \mu\text{g m}^{-3}$. In contrast, the impacts of the fires on PM_{2.5} AQ in Canberra are not seen until November and December. However, concentrations are much higher in Canberra, reaching $>100 \mu\text{g m}^{-3}$ in November and $>300 \mu\text{g m}^{-3}$ in December. PM_{2.5} AQ in Melbourne is affected latest, with PM_{2.5} concentrations reaching 50 to $>150 \mu\text{g m}^{-3}$ in December and January.

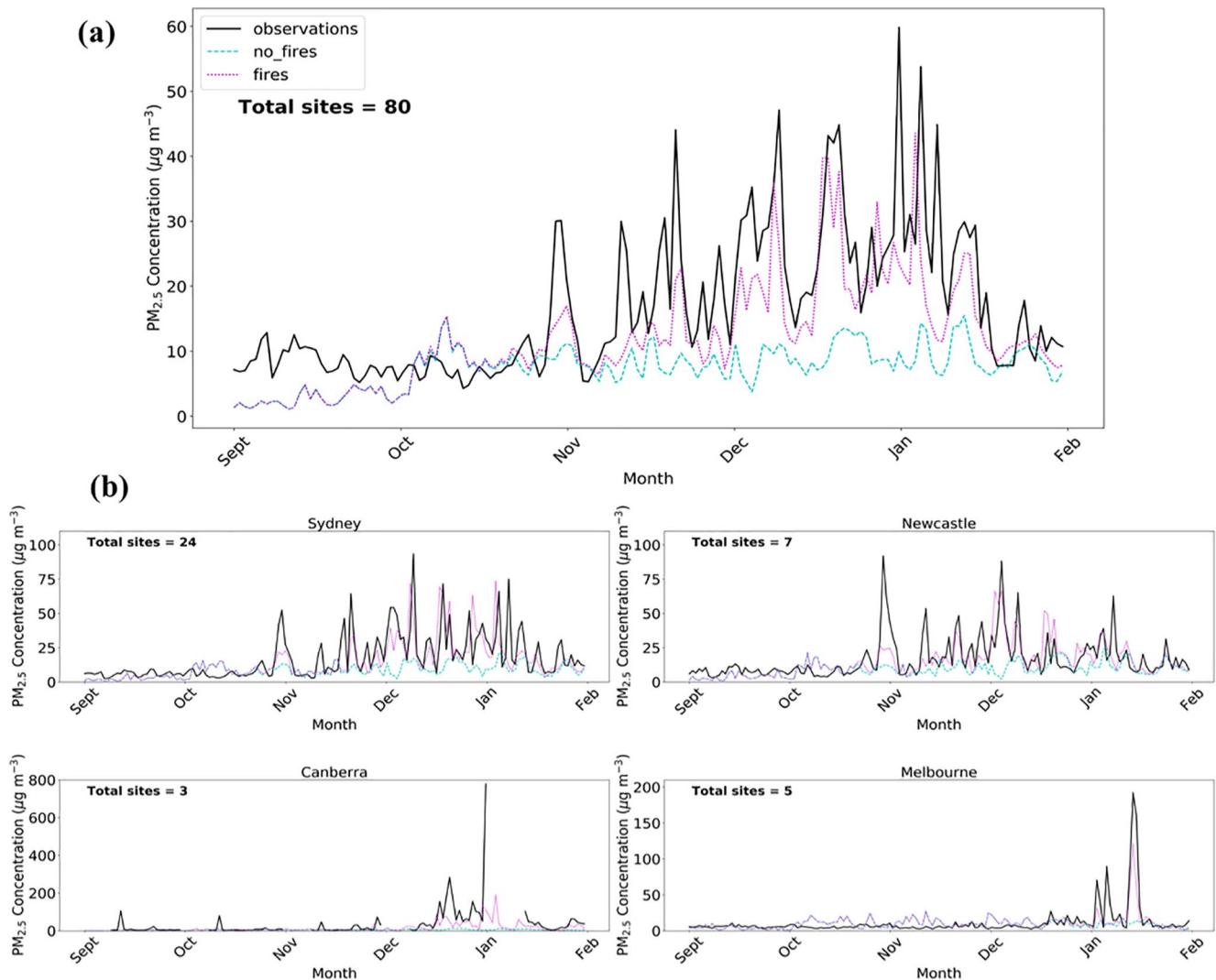


Figure 2. (a) Observed (black) and simulated (dotted magenta and dashed cyan) daily mean particulate matter with a diameter less than 2.5 µm (PM_{2.5}) concentrations. Simulations shown are no fires (dashed cyan) and fires (dotted magenta). The mean PM_{2.5} concentration from all 80 observational sites across eastern-Australia is shown for the model and observations. (b) The same as above but for individual cities (Sydney, Newcastle, Canberra, and Melbourne). The observed (black) and simulated (dotted magenta and dashed cyan) daily mean PM_{2.5} concentrations are shown for each city. The total number of observational sites in each city is also shown on the left of each panel.

3.2. Model Evaluation

Evaluation of the WRF-Chem model indicates that the model generally underestimates PM_{2.5} in early September (by ~70%) but then tends to overestimate PM_{2.5} (by ~30%) in early October (before the fires) across all sites (Figure 2). This is also generally true at city scale (Figure 2). During the fire period (late-October–November) there is a substantial enhancement in PM_{2.5} in both the observations and WRF-Chem fires simulation. The fires simulation captures the variability in PM_{2.5} observations reasonably well ($r = 0.53$), particularly compared to the no fires simulation ($r = 0.22$). The fires simulation also captures the concentrations observed in the peaks and ambient conditions well (RMSE = 24.1 µg m⁻³, NMB = -0.24), compared to the no fires simulation (RMSE = 27.3 µg m⁻³, NMB = -0.49) and the RMSE is better than the scaled fire emissions simulation [scaled_1.5] (RMSE = 25.0 µg m⁻³, NMB = -0.11), in which fire emissions between September and February were scaled by 1.5 (see Text S1 and Figure S4 in Supporting Information S1 for more details). The model performance is in line with previous modeling studies that estimated wildfire PM concentrations during other large wildfire events in Indonesia using WRF-Chem. Our model simulations show similar r and NMB values when compared with observed PM_{2.5} concentrations to

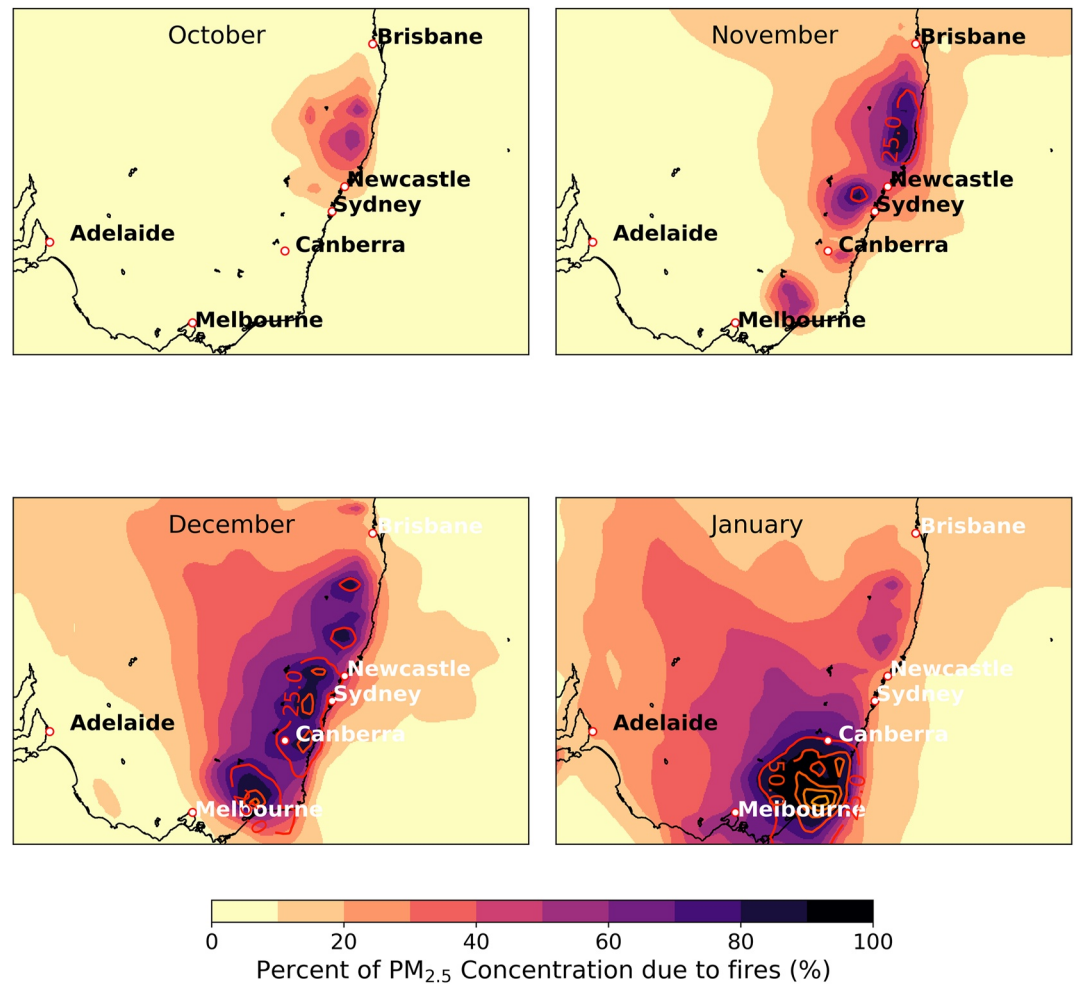


Figure 3. Monthly mean percentage of particulate matter with a diameter less than $2.5 \mu\text{m}$ ($\text{PM}_{2.5}$) attributable to fires, calculated as $\text{PM}_{2.5 \text{ fires}} - \text{PM}_{2.5 \text{ no fires}} / \text{PM}_{2.5 \text{ fires}}$ using the fires and no fires simulations. Monthly mean $\text{PM}_{2.5}$ concentrations from the fires simulation are also over plotted in contours for reference.

previous WRF-Chem studies focused on fires in Indonesia ($r = 0.51, 0.56$ and $\text{NMB} = -0.47, 0.18$) (Kiely et al., 2019, 2020) ($r = 0.55$ to 0.57 and $\text{NMB} = -0.24$ – -0.15) (Crippa et al., 2016). The model performs well in all of the cities, which have several observational sites (Sydney, Newcastle, and Melbourne), capturing the variability and magnitude of the peaks in $\text{PM}_{2.5}$ well. The model struggles to capture the magnitude of the $\text{PM}_{2.5}$ peaks observed in Canberra but this is likely due to the lack of observations (3 sites), meaning the model struggles to represent a small number of point measurements. $\text{PM}_{2.5}$ concentrations in cities for which there are many more observation locations (5–24 sites) are represented better by the model. The improvement in model performance in cities where there are multiple observations gives confidence in the ability of the model to represent the population exposure to $\text{PM}_{2.5}$ from the fires.

Monthly mean modeled $\text{PM}_{2.5}$ concentrations from the fires and no fire runs can be used to understand the impact of the bushfires on $\text{PM}_{2.5}$ concentrations across south-east Australia (Figure 3, and Figure S6 and S7 in Supporting Information S1). This indicates that although monthly mean concentrations were relatively low in October and November (monthly mean $\leq 25 \mu\text{g m}^{-3}$), a large fraction of $\text{PM}_{2.5}$ around Brisbane (20%–30%) and also Newcastle and Sydney (20%–100%) was from fires (Figure 3). This bushfire fraction increases in magnitude and spatial extent as the fires peak in December and January, when $>70\%$ of $\text{PM}_{2.5}$ is from fires over a large region including Melbourne, Canberra, Sydney, Newcastle and Brisbane (Figure 3).

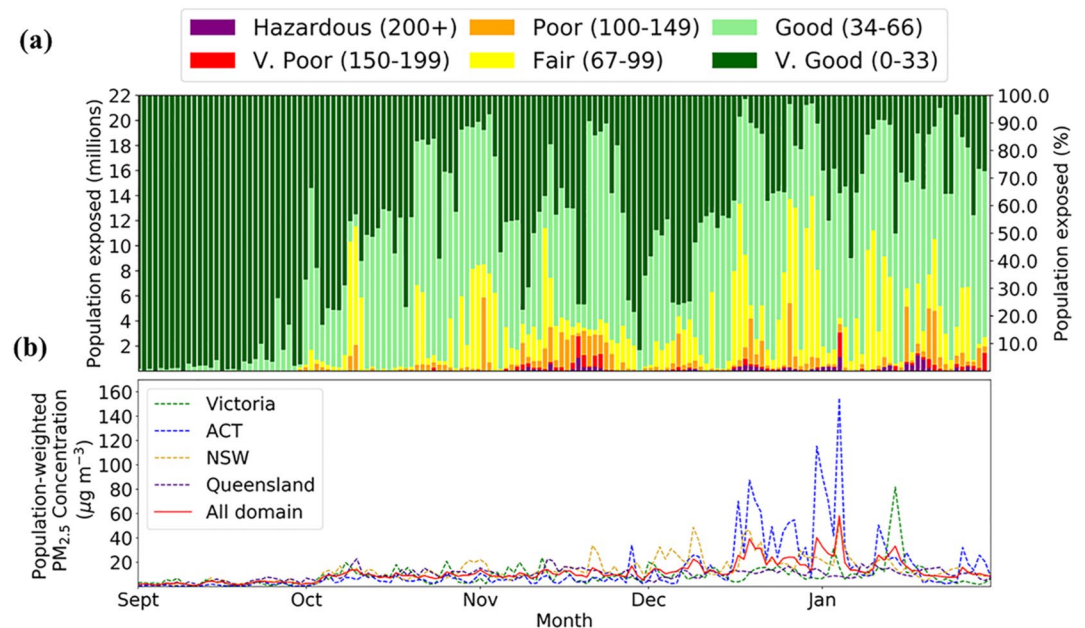


Figure 4. (a) Daily population exposure (in millions and %) to New South Wales Air Quality Index (AQI) values across eastern-Australia (fires simulation) between September 1 and January 31. AQI values correspond to particulate matter with a diameter less than $2.5 \mu\text{m}$ ($\text{PM}_{2.5}$) concentrations of 0–8.5 (V. Good), >8.5–16.75 (Good), >16.75–25 (Fair), >25–37.5 (Poor), >37.5–50 (V. Poor), >50 (Hazardous), all in $\mu\text{g m}^{-3}$. More information on how the AQI is calculated is available in Table S7 in Supporting Information S1. (b) Daily population-weighted bushfire $\text{PM}_{2.5}$ exposure (in $\mu\text{g m}^{-3}$) across all states in the model domain (red) and regionally for Victoria (green), Australian Capital Territory blue (yellow) and Queensland (purple) (fires-no fires simulation) between September 1 and January 31.

3.3. Air Quality Impacts

Combining simulated $\text{PM}_{2.5}$ concentrations with population data (at 1 km) allows the contribution of the fires to population exposure to poor AQ to be estimated across eastern-Australia (Figure 4a, Figure S8 in Supporting Information S1) and in individual cities (Figure 5a). Across eastern-Australia exposure to New South Wales Air Quality Index (AQI) values before the fires (in September and October) were dominated by “V.Good” and “Good” values (Figures 4a and Table 1 (Fires)). During September, on average, ~21.4 million people were exposed to “V. Good” and “Good” AQI concentrations (Table 1 (Fires)), while ~6,000 people were exposed to concentrations poorer than “Good” AQI. In October, there was an increase in the monthly mean population exposure to poor $\text{PM}_{2.5}$ AQ (“Poor,” “V.Poor” and “Hazardous” $\text{PM}_{2.5}$ AQI values) (Figure 4a), however overall monthly mean exposure to poor AQ remained low. Throughout November exposure to poor AQ increased, exposing 1.35 m people to “Poor” or “V.Poor” $\text{PM}_{2.5}$ AQI (Figure 4a and Table 1 (Fires)). Between November 1 and February 1 the average population exposed to “Poor,” “V.Poor,” and “Hazardous” $\text{PM}_{2.5}$ AQI values was ~1.5 m in November, 935,000 in December and ~1.3 m in January (Table 1 (Fires)). This equates to a population ~2 times the size of Canberra-Queanbeyan (~0.6 m) or almost half of the population of Brisbane (~3.5 m) being exposed to “Poor” or worse AQ on average from November to February.

By comparing the mean population AQI exposure (calculated as the daily population exposure to each AQI, subsequently averaged between September and February) during the bushfires to if there were no fires exposure to high AQI value can be attributed to the fires rather than as a result of other effects (e.g., long-range transport of $\text{PM}_{2.5}$). This indicates that in the fires (and no fires) simulation between September and February ~604,000 (~279,000) people were exposed to “Poor” AQI values, ~122,000 (~89,000) people to “V. Poor” AQI values and ~95,000 (~69,000) people to “Hazardous” AQI values. Therefore, the fires led to an additional ~437,000 people being exposed to “Poor” or worse AQI values on average (~279,000 exposed to “Poor,” 89,000 to “V.Poor” and 69,000 to “Hazardous” AQI values) across eastern Australia between September and February.

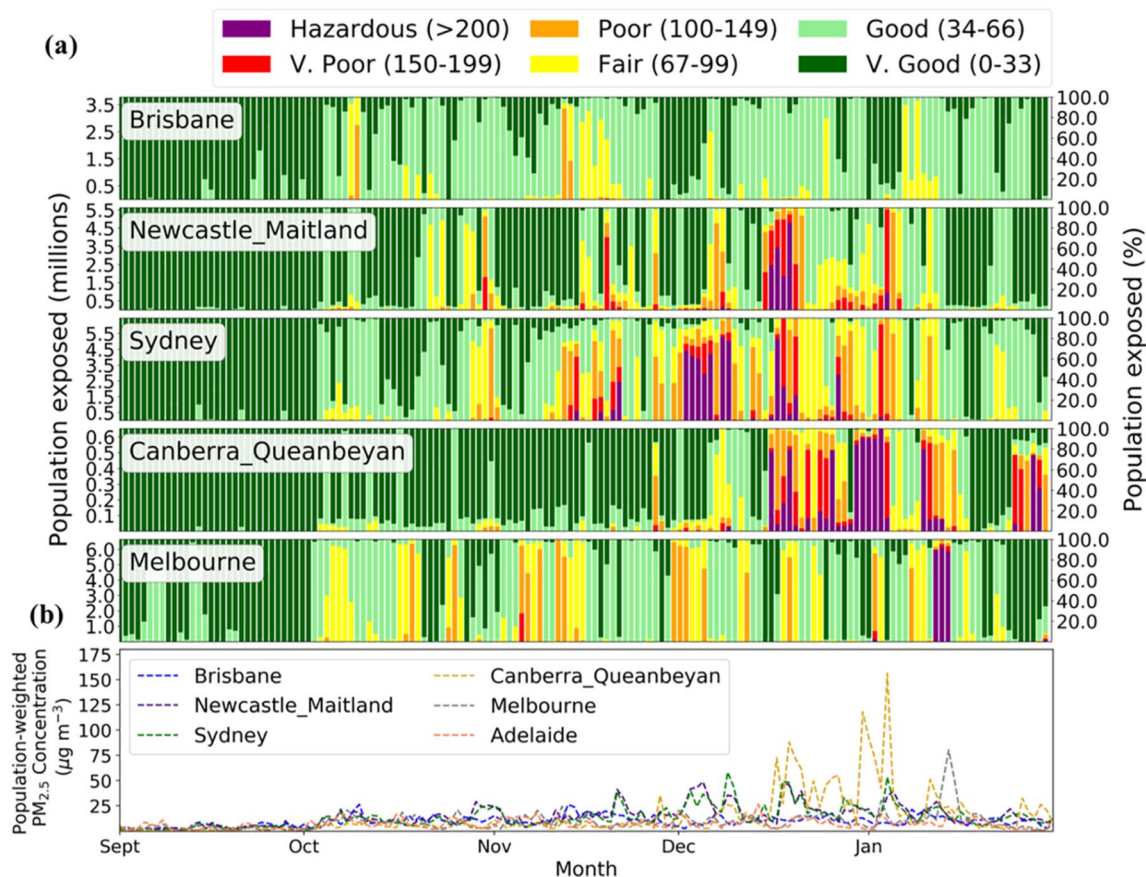


Figure 5. (a) Daily population exposure (in millions and % of total population) to New South Wales Air Quality Index (AQI) values in individual cities (Brisbane (Queensland), Sydney (NSW), Newcastle-Maitland (NSW), Canberra-Queanbeyan (ACT), and Melbourne (Victoria)) between September 1st and January 31. AQI values correspond to PM_{2.5} concentrations of 0–8.5 (V. Good), >8.5–16.75 (Good), >16.75–25 (Fair), >25–37.5 (Poor), >37.5–50 (V. Poor), >50 (Hazardous), all in $\mu\text{g m}^{-3}$. More information on how the AQI is calculated is available in Table S7 in Supporting Information S1. (b) Daily population-weighted bushfire PM_{2.5} concentration (in $\mu\text{g m}^{-3}$) in the cities of Brisbane (blue), Newcastle-Maitland (purple), Sydney (green), Canberra-Queanbeyan (yellow), Melbourne (gray), and Adelaide (orange) (fires-no fires simulation) between September 1 and January 31.

In order to understand the impact of poor AQ from the fires on the population, the bushfire PM_{2.5} concentration can be weighted by the total population in each region (population weighted bushfire PM_{2.5} – see Health Impact Assessment). We calculate the population-weighted bushfire PM_{2.5} concentration for the regions most severely affected by the fires (Figure 4b and Table 2 and Table S3 in Supporting Information S1). This indicates that the population in Australia Capital Territory (ACT) was exposed to the highest PM_{2.5} due to the fires (Table 2). Here, population-weighted bushfire PM_{2.5} concentrations reached $155.1 \mu\text{g m}^{-3}$ on January 4 and exceeded $100 \mu\text{g m}^{-3}$ on several days (Table 2). This is far above the maximum population-weighted PM_{2.5} concentrations in any of the other regions (Queensland ($22.9 \mu\text{g m}^{-3}$), New South Wales (NSW) ($53.4 \mu\text{g m}^{-3}$), Victoria ($81.8 \mu\text{g m}^{-3}$)) and far above the maximum between September 1 and January 31 across all regions, of $58.3 \mu\text{g m}^{-3}$ (Table 2). The mean population-weighted PM_{2.5} concentration between September and February across all regions was $11.6 \mu\text{g m}^{-3}$, with the highest mean population-weighted PM_{2.5} concentrations in ACT ($14.1 \mu\text{g m}^{-3}$) and NSW ($13.4 \mu\text{g m}^{-3}$) (Table 2). Comparing these results with Borchers Arriagada et al. (2020), population-weighted bushfire PM_{2.5} concentrations are considerably lower in this study (Table S3 in Supporting Information S1). This is evident from the difference in the mean and maximum population-weighted PM_{2.5} concentrations across all regions (mean: $11.6 \mu\text{g m}^{-3}$ vs. $23.7 \mu\text{g m}^{-3}$ and maximum: $58.3 \mu\text{g m}^{-3}$ vs. $98.5 \mu\text{g m}^{-3}$). The disparity is dominated by the large differences between estimates for ACT and Victoria (Table S3 in Supporting Information S1), where observations were relatively sparse.

Table 1

Monthly Population Exposure to PM_{2.5} AQI Values in the Fires and No Fires Simulation (Calculated as the Monthly Mean of Daily Sum Population Exposure)

Fires					
AQI	September (m)	October (m)	November (m)	December (m)	January (m)
V. Good	20.7	10.2	8.9	8.4	5.7
Good	0.73	9.6	8.6	9.0	12
Fair	0.014	2.1	2.4	3.8	3.2
Poor	6,000	0.30	1.1	0.75	0.79
V. Poor	41	0.012	0.26	0.08	0.25
Hazardous	0	93	0.12	0.11	0.24
No Fires					
AQI	September (m)	October (m)	November (m)	December (m)	January (m)
V. Good	20.7	10.8	12.2	11.5	7.8
Good	0.73	9.3	7.8	7.7	11.1
Fair	13,000	1.9	1.2	2.5	2.3
Poor	6,000	0.16	0.27	0.51	0.65
V. Poor	41	9,000	6,500	530	0.15
Hazardous	0	0	0	0	0.13

Note. More information on how the AQI is calculated in Table S7 in Supporting Information S1.

When individual cities are considered (Figure 5a) the effect of the southward shift of fires between October and January on population exposure to “Poor,” “V. Poor,” and “Hazardous” PM_{2.5} AQI can be clearly seen. In October, there is widespread exposure to “Poor” PM_{2.5} AQ. The effects of population exposure are largest in Brisbane, Newcastle-Maitland, Sydney and Melbourne with 93,000, 220,000, 49,000, and 468,000 people exposed to “Poor” or worse PM_{2.5} AQI values on average (Figure 5a and Table S2 in Supporting Information S1). The impacts of fires on PM_{2.5} AQ becomes most evident from November. During November average population exposure to “Poor,” “V. Poor,” and “Hazardous” PM_{2.5} AQ is evident in Sydney (112,000, 86,000, and 10,000 people exposed) and Newcastle-Maitland (235,000, 170,000, and 2,500 people exposed). Alongside this, in Canberra-Queanbeyan an average of 15,000, 1,100, and 174 people are exposed to “Poor,” “V.

Table 2

Mean and Maximum (September 1–January 31) Population-Weighted PM_{2.5} Concentrations for Regions and Cities in Eastern-Australia

Region	Mean population-weighted PM _{2.5} (μg m ⁻³)	Maximum population-weighted PM _{2.5} (μg m ⁻³)
Australian Capital Territory	14.1	155.1
New South Wales	13.4	53.4
Queensland	9.7	22.9
Victoria	9.1	81.8
All domain	11.6	58.3
City	Mean population-weighted PM _{2.5} (μg m ⁻³)	Maximum population-weighted PM _{2.5} (μg m ⁻³)
Brisbane	9.7	26.4
Newcastle-Maitland	14.3	48.7
Sydney	13.8	58.4
Canberra-Queanbeyan	14.2	156.2
Melbourne	9.0	80.5
Adelaide	7.0	26.5

Poor,” and “Hazardous” $PM_{2.5}$ AQI values in November. The pattern of increasing population exposure to poor $PM_{2.5}$ AQ continues in December, as the fires intensify, with a clear southward shift (Figure 5a). Populations in Sydney, Newcastle-Maitland, and Canberra-Queanbeyan continue to be exposed to “Poor” and worse AQ. This leads to 3.6, 1.7, and 237,000 people being exposed to “Poor” or worse AQ in Sydney, Newcastle-Maitland, and Canberra-Queanbeyan, respectively, on average in December (Table S2 in Supporting Information S1). During this time in Brisbane, Melbourne and Adelaide ~5,000, 1.1 m and 53,000 people on average are exposed to “Poor” or worse AQ. Finally, in January, the southward shift in fires continues, with a clear decrease in exposure to “Poor” or worse AQI in Brisbane, Sydney, and Newcastle-Maitland but increases in monthly mean exposure to “Poor” AQ in Canberra-Queanbeyan, Melbourne and Adelaide. This leads to 286,000, 979,000, and ~48,000 people being exposed to “Poor,” “V. Poor,” and “Hazardous” $PM_{2.5}$ AQI values in Canberra-Queanbeyan, Melbourne and Adelaide on average (Table S2 in Supporting Information S1). Despite reductions in the total population exposed to hazardous AQI values in Newcastle-Maitland and Sydney, widespread population exposure to “Poor,” “V. Poor,” and “Hazardous” $PM_{2.5}$ AQI values continues during January. On average 515,000 and ~820,000 people are exposed to “Poor,” “V. Poor,” and “Hazardous” $PM_{2.5}$ AQI values in Newcastle-Maitland and Sydney in January (Table S2 in Supporting Information S1).

Population-weighted bushfire $PM_{2.5}$ (fires — no fires) for individual cities can be used to identify the cities most severely affected by bushfire-sourced $PM_{2.5}$ (Figures 5b and Table 2 and Figure S8 in Supporting Information S1). In line with the region population-weighted $PM_{2.5}$ concentrations, Canberra-Queanbeyan (ACT) is affected most severely by $PM_{2.5}$ from the fires. Population-weighted $PM_{2.5}$ concentrations in Canberra-Queanbeyan reach $156.2 \mu\text{g m}^{-3}$ and average $14.2 \mu\text{g m}^{-3}$ between September 1 and January 31 (Table 2). The maximum population-weighted $PM_{2.5}$ concentrations in Sydney ($58.4 \mu\text{g m}^{-3}$) and Newcastle-Maitland ($48.7 \mu\text{g m}^{-3}$) is much below Canberra-Queanbeyan (Table 2). However, as a result of the prolonged exposure to poor AQ in Sydney and Newcastle-Maitland, the mean population-weighted $PM_{2.5}$ concentrations in both cities ($13.8 \mu\text{g m}^{-3}$ and $14.3 \mu\text{g m}^{-3}$) are similar to Canberra-Queanbeyan (Table 2).

These results clearly indicate widespread population exposure to dangerous $PM_{2.5}$ AQI levels throughout November, December and January. This is likely to have a large impact on public health due to short-term exposure to high $PM_{2.5}$ concentrations. We estimate these effects in the next section.

3.4. Health Impacts

Using the World Health Organisation (2013) concentration response function, the number of deaths brought forward due to $PM_{2.5}$ from the fires between October 1 and January 31 can be estimated using the concentration of $PM_{2.5}$ due to fires (i.e., the difference in $PM_{2.5}$ concentrations between the fires and no fires simulations) (Figure 6). This indicates the impact of short-term exposure to bushfire $PM_{2.5}$ has a substantial impact on health from mid-October to mid-January (Figure 6a). In total 171 (95% CI: 64–277) deaths were brought forward as a result of short-term exposure to bushfire $PM_{2.5}$ (Table S5 in Supporting Information S1) and 624 (95% CI: 230–1008) from short-term exposure to all $PM_{2.5}$. Therefore, the bushfires accounted for almost 30% of the deaths brought forward from short-term exposure to $PM_{2.5}$ during this period. This represents an increase of 38%, compared to if there were no fires.

Regionally, the health impact of exposure to $PM_{2.5}$ was largest in New South Wales (NSW), Queensland and Victoria (Figure 6b). We estimate that short-term exposure to all $PM_{2.5}$ between October and February led to 287 (95% CI: 107–463), 112 (95% CI: 41–181), and 155 (95% CI: 57–250) deaths being brought forward in NSW, Queensland, and Victoria, respectively. Of these deaths, 109 (95% CI: 41–176), 15 (95% CI: 5–24) and 35 (95% CI: 13–56) deaths brought forward were due to short-term exposure to bushfires $PM_{2.5}$ (Table S6 in Supporting Information S1). This indicates the bushfires accounted for 38%, 13%, and 30% of the total deaths brought forward by short-term exposure to bushfire $PM_{2.5}$ in NSW, Queensland and Victoria, respectively. Comparing our estimates with the results of Borchers Arriagada et al. (2020) and Ryan et al. (2021) (Figure 6b) the estimates in this study are within the range of both studies in NSW. We estimate 109 (95% CI: 41–176) deaths are brought forward by short-term exposure to bushfire $PM_{2.5}$, while Borchers Arriagada et al. (2020) estimate 219 (95% CI: 81–357) and Ryan et al. (2021) estimate 152.1 (95% CI: 95–209). Our results lie below the lower end of estimates in Victoria at 35 (95% CI: 13–56) deaths brought forward due to short-term exposure to bushfire $PM_{2.5}$. This is considerably lower than Borchers Arriagada et al. (2020) estimate of

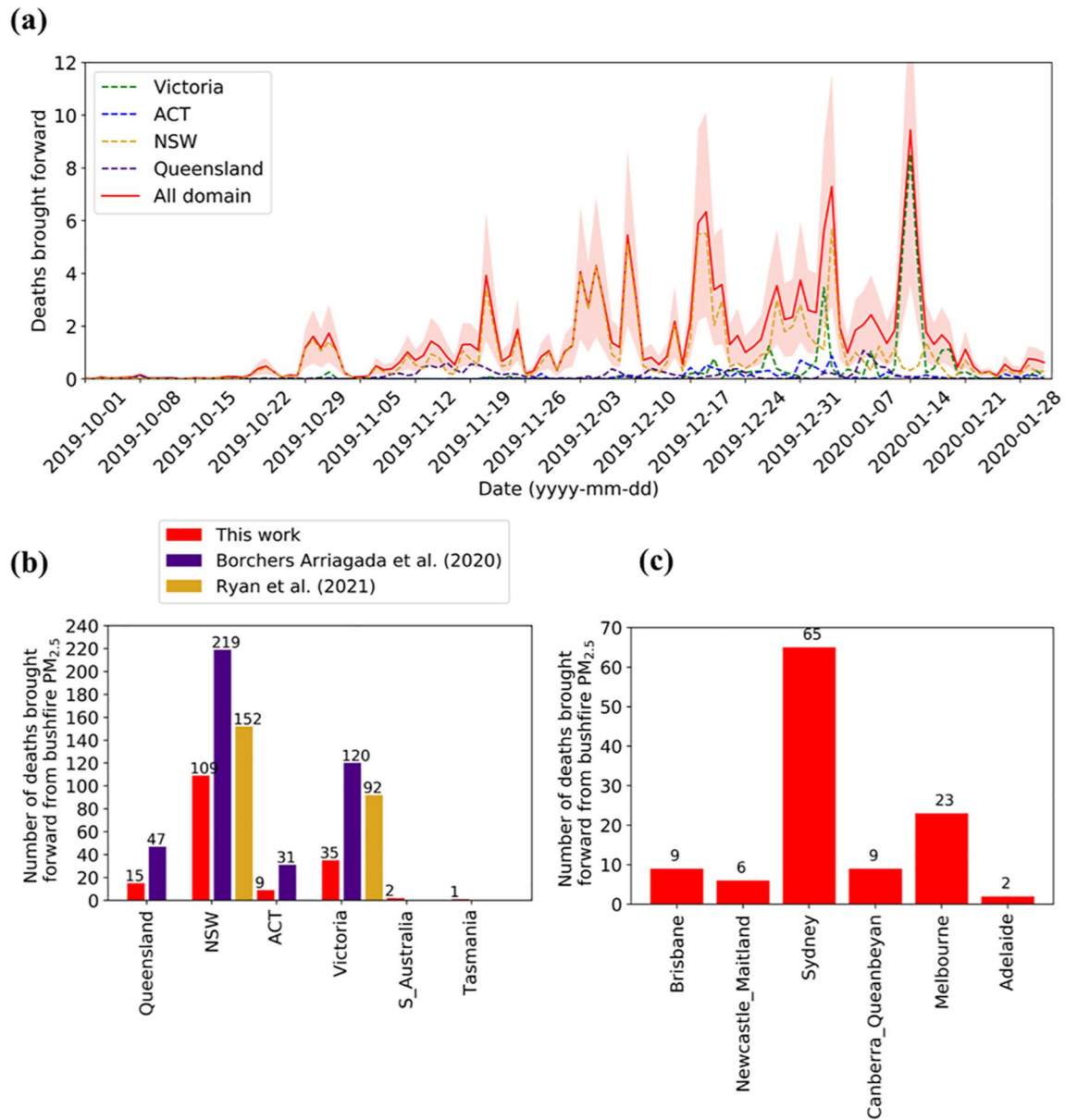


Figure 6. (a) Estimated increase in the number of deaths brought forward across model domain (red) and the regions of Victoria (green), Australia Capital Territory (ACT) (blue), New South Wales (NSW) (yellow), and Queensland (purple) due to particulate matter with a diameter less than 2.5 μm ($\text{PM}_{2.5}$) from bushfires (fires only) between October 1 and January 31. Shading indicates the 95% confidence intervals of the estimate. The number of deaths brought forward due to bushfire $\text{PM}_{2.5}$ (fires only) between October 1 and January 31 is also broken down by region (b) and city (c) and the total number of deaths is shown above the bars. The estimated number of deaths brought forward in each region (b) due to bushfire $\text{PM}_{2.5}$ (fires only) (red) in this study are compared to the Borchers Arriagada et al. (2020) (indigo) and Ryan et al. (2021) (gold) estimates for the same period.

120 (95% CI: 44–195) and Ryan et al. (2021) estimate of 92 (95% CI: 57–126) deaths brought forward due to short-term exposure to bushfire $\text{PM}_{2.5}$. All three studies use the same population, baseline mortality datasets and concentration-response function. Therefore, the disparity in results between the studies is likely due to a number of other factors. First, our study uses modeled $\text{PM}_{2.5}$ concentrations, rather than observations. Since the model generally underestimates $\text{PM}_{2.5}$ concentrations, the overall health impact estimated is likely to be underestimated due to a reduction in population exposure to $\text{PM}_{2.5}$. Second, the bushfire fraction of the total $\text{PM}_{2.5}$ mass could be overestimated in the Borchers Arriagada et al. (2020) study due the use of monthly mean historical $\text{PM}_{2.5}$ concentrations to account for the no fire fraction of $\text{PM}_{2.5}$. This would not account for the effect of meteorology on ambient $\text{PM}_{2.5}$, which may be important given the strong positive

Indian Ocean Dipole that year. If ambient $PM_{2.5}$ concentrations without fires were underestimated due to this there would be a resulting overestimation in the health impact of bushfire $PM_{2.5}$ (since $PM_{2.5}^{FIRES\ ONLY} = PM_{2.5}^{ALL} - PM_{2.5}^{NO\ FIRES}$). Ryan et al. (2021) used a random forest model to simulate the non-bushfire $PM_{2.5}$ fraction, which accounted for the effect of meteorology on ambient $PM_{2.5}$ concentrations, like our model. Their estimate is also lower than Borchers Arriagada et al. (2020), further supporting this.

When individual cities are considered in the health impact assessment it becomes clear that the health impact from short-term exposure to bushfire $PM_{2.5}$ is concentrated in cities with high populations, where $PM_{2.5}$ concentrations due to fires were high (Figure 6c). Of the large cities we investigated, the impact of short-term exposure to bushfire $PM_{2.5}$ on mortality was largest in Sydney (65 (95% CI: 24–105)), Melbourne (23 (95% CI: 9–38)), and Canberra-Queanbeyan (9 (95% CI: 4–14)) (Figure 6, Table S6 in Supporting Information S1). In these cities short-term exposure to bushfire $PM_{2.5}$ accounted for 36%, 20%, and 64% of the total deaths brought forward from short-term exposure to $PM_{2.5}$, respectively.

4. Conclusions

We use the WRF-Chem regional air quality model to estimate the impact of the 2019/2020 Australian bushfires across eastern Australia, complementing the work of Borchers Arriagada et al. (2020) and Ryan et al. (2021), which were based solely on analysis of $PM_{2.5}$ observations. FINN fire emissions indicate $PM_{2.5}$ emissions from the 2019/2020 bushfires were unprecedented. Around 1 Tg of $PM_{2.5}$ was emitted from the fires during 2019 and ~0.3 Tg between January and February 2020. This is likely due to the high levels of dry fuel availability across the region during 2019 (van Oldenborgh et al., 2020).

Two model simulations were performed (a) with FINN fire emissions (fires) and (b) without FINN fire emissions (no fires), which allowed the impact of the bushfires on $PM_{2.5}$ AQ and health to be quantified. Simulated $PM_{2.5}$ concentrations from the fires simulation reproduced observed daily mean concentrations relatively well but with a low bias ($r = 0.53$, $RMSE = 24.1 \mu g m^{-3}$, $NMB = -0.24$, $NMAE = 0.65$). Despite this, modeled $PM_{2.5}$ concentrations captured the variability and magnitude of peaks seen in the observations across eastern-Australia and for specific cities.

We find that between September and February large proportions of the population were exposed to dangerous (“Poor,” “V.Poor,” and “Hazardous”) air quality levels. In total, the fires led to an additional ~437,000 people being exposed to “Poor” or worse AQI values on average (~279,000 exposed to “Poor,” 89,000 to “V.Poor” and 69,000 to “Hazardous” AQI values) across eastern Australia between September and February, compared to if there were no fires. The impact of the bushfires on AQ was concentrated in the cities of Sydney, Newcastle-Maitland and Canberra-Queanbeyan during November, December and, also in Melbourne, in January. While, generally Brisbane and Adelaide were less severely affected by the fires.

We estimate the impacts of short-term exposure to $PM_{2.5}$ from bushfires on all-cause, all-age mortality across eastern-Australia, regionally and in individual cities using a short-term exposure response function (World Health Organization, 2013). Our estimate indicates that between October and February 171 (95% CI: 64–277) deaths were brought forward due to short-term exposure to bushfire $PM_{2.5}$, 624 (95% CI: 230–1,008) due to all $PM_{2.5}$ and 456 (95% CI: 169–738) if there were no fires. The health impact due to short-term exposure to bushfire $PM_{2.5}$ was largest in New South Wales, Queensland, and Victoria with 109 (95% CI: 41–176), 15 (95% CI: 5–24), and 35 (95% CI: 13–56) deaths brought forward in these regions (287 (95% CI: 107–463)), 112 (95% CI: 41–181), and 155 (95% CI: 57–250) all $PM_{2.5}$), respectively. Our results lie within the range of estimated health impacts due to short-term exposure to bushfire $PM_{2.5}$ from both Borchers Arriagada et al. (2020) and Ryan et al. (2021) for New South Wales but below the lower limit for other regions, such as Victoria. This is most likely due to differences in how ambient $PM_{2.5}$ (and therefore bushfire $PM_{2.5}$) was estimated in each study and also differences in the estimated population-weighted bushfire $PM_{2.5}$ concentrations. However, this study builds upon previous work by using an atmospheric chemistry transport model to simulate $PM_{2.5}$ concentrations, while accounting for real time meteorological conditions and atmospheric processes, and calculating explicitly the $PM_{2.5}$ increment due to the fires. At a city-level, the health impacts of $PM_{2.5}$ exposure due to bushfires were concentrated in the cities with large populations and high $PM_{2.5}$ concentrations due to bushfires. The highest number of deaths brought forward due to short-term bushfire $PM_{2.5}$ exposure were in Sydney (65 (95% CI: 24–105)), Melbourne (23 (95% CI: 9–38))

and Canberra-Queanbeyan (9 (95% CI: 4–14). In these cities short-term exposure to bushfire PM_{2.5} accounted for 36%, 20%, and 64% of the total deaths brought forward from short-term exposure to PM_{2.5}.

This work confirms that there was a substantial AQ and health impact across eastern-Australia from the 2019/2020 bushfires. Our study only considered mortality, therefore the full health impact of exposure to PM_{2.5} is likely to be higher and requires further studies addressing the impacts on hospital admissions, ambulance call outs and primary health care visits. Alongside this, the impact of other pollutants on health could also be quantified. In the future, further work is required to characterize the health impacts of exposure to pollutants from wildfires. This would allow for more comprehensive estimates of the health impacts associated with population exposure. Finally, with more dry years like 2019/2020 projected to occur in the future due to climate change the impact of wildfires such as 2019/2020 are likely to be seen again. Therefore, fire risk management policies should be developed further to consider the impact of climate change on wildfire frequency and intensity across the country.

Conflict of Interest

The authors declare no conflicts of interest relevant to this study.

Data Availability Statement

Observations of PM_{2.5} were accessed from the <https://www.dpie.nsw.gov.au/air-quality/air-quality-concentration-data-updated-hourly>, <https://discover.data.vic.gov.au/dataset/epa-air-watch-all-sites-air-quality-hourly-averages-yearly/historical>, <https://www.data.qld.gov.au/dataset/air-quality-monitoring-2019/resource/c9ecf021-faa4-4d5a-93c7-7460c083d682>, and <https://www.data.act.gov.au/Environment/Air-Quality-Monitoring-Data/94a5-zqnn>. Gridded population data for 2018 was accessed from the Australia Bureau of Statistics <https://www.abs.gov.au/AUSSTATS/abs@.nsf/DetailsPage/3218.02017-18?OpenDocument>. All-cause mortality data for 2018 was taken from the Australia Bureau of Statistics http://stat.data.abs.gov.au/Index.aspx?DataSetCode=DEATHS_AGESPECIFIC_OCCURENCEYEAR. The authors acknowledge use of the Weather Research and Forecasting model coupled with Chemistry preprocessor tool mozbc, fire_emiss, bio_emiss and anthro_emis provided by the Atmospheric Chemistry Observations and Modeling Lab (ACOM) of NCAR. The authors acknowledge use of the postprocessing script “wrfout_to_cf.ncl” created by Mark Seefeldt at the University of Colorado at Boulder (http://foehn.colorado.edu/wrfout_to_cf/). The Supporting Information S1 contains all results and further information on our analysis. As far as we are aware there are no competing financial interests. Code to setup and run WRFChem (using WRFotron version 2.0) are available through Conibear and Knot (2020). WRF-Chem simulation data are available from the Research Data Leeds Repository (<https://doi.org/10.5518/988>).

Acknowledgment

This work was supported by the UK Natural Environment Research Council (NERC) by providing funding for the National Centre for Earth Observation (NCEO), Grant No. NE/R016518/1.

References

- Akagi, S. K., Yokelson, R. J., Wiedinmyer, C., Alvarado, M. J., Reid, J. S., Karl, T., et al. (2011). Emission factors for open and domestic biomass burning for use in atmospheric models. *Atmospheric Chemistry and Physics*, 11, 4039–4072. <https://doi.org/10.5194/acp-11-4039-2011>
- Andreae, M. O., & Melret, P. (2001). Emission of trace gases and aerosols from biomass burning. *Global Biogeochemical Cycles*, 15, 955–966. <https://doi.org/10.1029/2000GB001382>
- Archer-Nicholls, S., Lowe, D., Darbyshire, E., Morgan, W. T., Bela, M. M., Pereira, G., et al. (2015). Characterising Brazilian biomass burning emissions using WRF-chem with MOSAIC sectional aerosol. *Geoscientific Model Development*, 8, 549–577. <https://doi.org/10.5194/gmd-8-549-2015>
- Australian Bureau of Meteorology (2019a). Southern annular mode [WWW Document]. Retrieved from <http://www.bom.gov.au/climate/about/?bookmark=sam>
- Australian Bureau of Meteorology (2019b). Tracking Australia's climate through 2019 [WWW Document]. Retrieved from <http://www.bom.gov.au/climate/updates/articles/a036.shtml>
- Australian Bureau of Meteorology (2020). Australian climate influences: IOD [WWW Document]. Retrieved from <http://www.bom.gov.au/climate/about/?bookmark=iod>
- Australian Bureau of Statistics (2019). Regional population growth, Australia, 2017–18 [WWW Document]. Retrieved from <https://www.abs.gov.au/AUSSTATS/abs@.nsf/DetailsPage/3218.02017-18?OpenDocument>
- Australian Bureau of Statistics (2020). Deaths, year of occurrence, age at death, age-specific death rates, sex, states, territories and Australia [WWW Document]. Retrieved from http://stat.data.abs.gov.au/Index.aspx?DataSetCode=DEATHS_AGESPECIFIC_OCCURENCEYEAR
- Black, C., Tesfaigzi, Y., Bassein, J. A., & Miller, L. A. (2017). Wildfire smoke exposure and human health: Significant gaps in research for a growing public health issue. *Environmental Toxicology and Pharmacology*, 55, 186–195. <https://doi.org/10.1016/j.etap.2017.08.022>

- Borchers Arriagada, N., Palmer, A. J., Bowman, D. M. J. S., Morgan, G. G., Jalaludin, B. B., Johnston, F. H. (2020). Unprecedented smoke-related health burden associated with the 2019–20 bushfires in eastern Australia. *Medical Journal of Australia*, <https://doi.org/10.5694/mja2.50545>
- Brew, N., Richards, L., Smith, L. (2020). 2019–2020 Australian bushfires—frequently asked questions: A quick guide.
- Conibear, L., Butt, E., Knote, C., Arnold, S., & Spracklen, D. (2018a). Residential energy use emissions dominate health impacts from exposure to ambient particulate matter in India. *Nature Communications*, 9, 1–9. <https://doi.org/10.1038/s41467-018-02986-7>
- Conibear, L., Butt, E., Knote, C., Arnold, S., & Spracklen, D. (2018b). Stringent emission control policies can provide large improvements in air quality and public health in India. *GeoHealth*, 2, 196–211. <https://doi.org/10.1029/2018gh000139>
- Conibear, L., Butt, E., Knote, C., Spracklen, D., & Arnold, S. (2018). Current and future disease burden from ambient ozone exposure in India. *GeoHealth*, 2, 334–355. <https://doi.org/10.1029/2018gh000168>
- Conibear, L., & Knote, C. (2020). WRFotron [WWW Document]. Retrieved from <https://agupubs.onlinelibrary.wiley.com/doi/full/10.1029/2021GH000391#gh2231-bib-0010>
- Crippa, P., Castruccio, S., Archer-Nicholls, S., Lebron, G., Kuwata, M., Thota, A., et al. (2016). Population exposure to hazardous air quality due to the 2015 fires in equatorial Asia. *Scientific Reports*, 6, 1–9. <https://doi.org/10.1038/srep37074>
- Delfino, R. J., Brummel, S., Wu, J., Stern, H., Ostro, B., Lipsett, M., et al. (2009). The relationship of respiratory and cardiovascular hospital admissions to the southern California wildfires of 2003. *Occupational and Environmental Medicine*, 66, 189–197. <https://doi.org/10.1136/oem.2008.041376>
- Emmons, L. K., Walters, S., Hess, P. G., Lamarque, J.-F., Pfister, G. G., Fillmore, D., et al. (2009). Description and evaluation of the model for ozone and related chemical tracers, version 4 (MOZART-4). *Geoscientific Model Development Discussions*, 2, 1157–1213. <https://doi.org/10.5194/gmdd-2-1157-2009>
- Faustini, A., Alessandrini, E. R., Pey, J., Perez, N., Samoli, E., Querol, X., et al. (2015). Short-term effects of particulate matter on mortality during forest fires in Southern Europe: Results of the MED-PARTICLES project. *Occupational and Environmental Medicine*, 72, 323–329. <https://doi.org/10.1136/oemed-2014-102459>
- Freitas, S. R., Longo, K. M., Chatfield, R., Latham, D., Silva Dias, M. A. F., Andreae, M. O., et al. (2007). Including the sub-grid scale plume rise of vegetation fires in low resolution atmospheric transport models. *Atmospheric Chemistry and Physics*, 7, 3385–3398. <https://doi.org/10.5194/acp-7-3385-2007>
- Hoelzemann, J. J., Schultz, M. G., Brasseur, G. P., Granier, C., & Simon, M. (2004). Global wildland fire emission model (GWEM): Evaluating the use of global area burnt satellite data. *Journal of Geophysical Research*, 109, 14–18. <https://doi.org/10.1029/2003JD003666>
- Hoffmann, L., Günther, G., Li, D., Stein, O., Wu, X., Griessbach, S., et al. (2018). From ERA-interim to ERA5: Considerable impact of ECMWF's next-generation reanalysis on lagrangian transport simulations. *Atmospheric Chemistry and Physics Discussions*, 1–38. <https://doi.org/10.5194/acp-2018-1199>
- Holgate, S. (1998). *Quantification of the effects of Air pollution on health in the United Kingdom*: The Stationary Office.
- Janssens-Maenhout, G., Crippa, M., Guizzardi, D., Dentener, F., Muntean, M., Pouliot, G., et al. (2015). HTAP-v2.2: A mosaic of regional and global emission grid maps for 2008 and 2010 to study hemispheric transport of air pollution. *Atmospheric Chemistry and Physics*, 15, 11411–11432. <https://doi.org/10.5194/acp-15-11411-2015>
- Johnston, F., Hanigan, I., Henderson, S., Morgan, G., & Bowman, D. (2011). Extreme air pollution events from bushfires and dust storms and their association with mortality in Sydney, Australia 1994–2007. *Environmental Research*, 111, 811–816. <https://doi.org/10.1016/j.envres.2011.05.007>
- Johnston, F. H., Henderson, S. B., Chen, Y., Marlier, M., DeFries, R. S., Kinney, P., et al. (2012). Estimated global mortality attributable to smoke from landscape fires. *Environmental Health Perspectives*, 120, 695–701. <https://doi.org/10.1289/ehp.1104422>
- Kiely, L., Spracklen, D. V., Wiedinmyer, C., Conibear, L., Reddington, C. L., Archer-Nicholls, S., et al. (2019). New estimate of particulate emissions from Indonesian peat fires in 2015. *Atmospheric Chemistry and Physics*, 19, 11105–11121. <https://doi.org/10.5194/acp-19-11105-2019>
- Kiely, L., Spracklen, D. V., Wiedinmyer, C., Conibear, L. A., Reddington, C. L., Arnold, S. R., et al. (2020). Air quality and health impacts of vegetation and peat fires in Equatorial Asia during 2004–2015. *Environmental Research Letters*, <https://doi.org/10.1088/1748-9326/ab9a6c>
- Lelieveld, J., Evans, J. S., Fnais, M., Giannadaki, D., & Pozzer, A. (2015). The contribution of outdoor air pollution sources to premature mortality on a global scale. *Nature*, 525, 367–371. <https://doi.org/10.1038/nature15371>
- Liu, J. C., Pereira, G., Uhl, S. A., Bravo, M. A., & Bell, M. L. (2015). A systematic review of the physical health impacts from non-occupational exposure to wildfire smoke. *Environmental Research*, 136, 120–132. <https://doi.org/10.1016/j.envres.2014.10.015>
- Lucas, C., Hennessy, K., Mills, G., Bathols, J. (2007). Bushfire weather in southeast Australia: Recent trends and projected climate change impacts. In *Consultancy Report Prepared for The Climate Institute of Australia* 84.
- Macintyre, H. L., Heaviside, C., Neal, L. S., Agnew, P., Thornes, J., & Vardoulakis, S. (2016). Mortality and emergency hospitalizations associated with atmospheric particulate matter episodes across the UK in spring 2014. *Environment International*, 97, 108–116. <https://doi.org/10.1016/j.envint.2016.07.018>
- Marsh, D. R., Mills, M. J., Kinnison, D. E., Lamarque, J. F., Calvo, N., & Polvani, L. M. (2013). Climate change from 1850 to 2005 simulated in CESM1 (WACCM). *Journal of Climate*, 26, 7372–7391. <https://doi.org/10.1175/JCLI-D-12-00558.1>
- McMeeking, G. R. (2008). *The optical, chemical, and physical properties of aerosols and gases emitted by the laboratory combustion of wildland fires* 321.
- Naeher, L. P., Brauer, M., Lipsett, M., Zelikoff, J. T., Simpson, C. D., Koenig, J. Q., & Smith, K. R. (2007). Woodsmoke health effects: A review. *Inhalation Toxicology*, 19, 67–106. <https://doi.org/10.1080/08958370600985875>
- Olivier, J., Peters, J., Granier, C., Pétron, G., Müller, J., & Wallens, S. (2003). *Present and future surface emissions of atmospheric compounds*.
- Reddington, C., Conibear, L., Knote, C., Silver, B., Li, Y., Chan, C., et al. (2019). Exploring the impacts of anthropogenic emission sectors on PM_{2.5} and human health in South and East Asia. *Atmospheric Chemistry and Physics*, 19, 11887–11910. <https://doi.org/10.5194/acp-19-11887-2019>
- Reid, C. E., Brauer, M., Johnston, F. H., Jerrett, M., Balmes, J. R., Elliott, C. T. E., et al. (2016). Critical review of health impacts of wildfire smoke exposure. *Environmental Health Perspectives*, 124, 1334–1343. <https://doi.org/10.1289/ehp.1409277>
- Ryan, R. G., Silver, J. D., & Schofield, R. (2021). Air quality and health impact of 2019–20 black summer megafires and COVID-19 lockdown in Melbourne and Sydney, Australia. *Environmental Pollution*, 274, 116498. <https://doi.org/10.1016/j.envpol.2021.116498>
- Schmidt, A., Ostro, B., Carslaw, K. S., Wilson, M., Thordarson, T., Mann, G. W., & Simmons, A. J. (2011). Excess mortality in Europe following a future Laki-style Icelandic eruption. *Proceedings of the National Academy of Sciences of the United States of America*, 108, 15710–15715. <https://doi.org/10.1073/pnas.1108569108>

- Silver, B., Conibear, L., Reddington, C., Knote, C., Arnold, S., & Spracklen, D. (2020). Pollutant emission reductions deliver decreased PM_{2.5}-caused mortality across China during 2015–2017. *Atmospheric Chemistry and Physics*, 2017, 1–18. <https://doi.org/10.5194/acp-2019-1141>
- Sutton, M. A., van Grinsven, H., Billen, G., Bleeker, A., Bouwman, A. F., Bull, K., et al. (2011). Summary for policy makers. *European Nitrogen Assessment*. <https://doi.org/10.1017/cbo9780511976988.002>
- UCAR (2020a). WACCM download [WWW Document]. Retrieved from <https://www.acom.ucar.edu/waccm/download.shtml>
- UCAR (2020b). WRF-chem MOZART-4 download [WWW Document]. Retrieved from <https://www.acom.ucar.edu/wrf-chem/mozart.shtml>
- van Oldenborgh, G. J., Krikken, F., Lewis, S., Leach, N., Lehner, F., Saunders, K., et al. (2020). Attribution of the Australian bushfire risk to anthropogenic climate change. *Natural Hazards and Earth System Sciences*, 1–46. <https://doi.org/10.5194/nhess-2020-69>
- Verzoni, A. (2021). *Wildlife toll* [WWW Document]. National Fire Protection Association.
- Wiedinmyer, C., Akagi, S. K., Yokelson, R. J., Emmons, L. K., Al-Saadi, J. A., Orlando, J. J., & Soja, A. J. (2011). The fire INventory from NCAR (FINN): A high resolution global model to estimate the emissions from open burning. *Geoscientific Model Development*, 4, 625–641. <https://doi.org/10.5194/gmd-4-625-2011>
- Wintle, B. A., Legge, S., & Woinarski, J. C. Z. (2020). After the megafires: What next for Australian wildlife? *Trends in Ecology & Evolution*, 35, 753–757. <https://doi.org/10.1016/j.tree.2020.06.009>
- World Health Organization (2013). *Health risks of air pollution in Europe — HRAPIE project*. World Health Organ. 60.
- Zanobetti, A., & Schwartz, J. (2009). The effect of fine and coarse particulate air pollution on mortality: A national analysis. *Environment Health Perspectives*, 117, 898–903. <https://doi.org/10.1289/ehp.0800108>
- Zaveri, R. A., Easter, R. C., Fast, J. D., & Peters, L. K. (2008). Model for simulating aerosol interactions and chemistry (MOSAIC). *Journal of Geophysical Research*, 113, 1–29. <https://doi.org/10.1029/2007JD008782>

Reference From the Supporting Information

- Liu, T., Mickley, L. J., Marlier, M. E., DeFries, R. S., Khan, M. F., Latif, M. T., & Karambelas, A. (2020). Diagnosing spatial biases and uncertainties in global fire emissions inventories: Indonesia as regional case study. *Remote Sensing Environment*, 237, 111557. <https://doi.org/10.1016/j.rse.2019.111557>